Clinical Biomechanics xxx (xxxx) xxx

Contents lists available at ScienceDirect

Clinical Biomechanics

journal homepage: www.elsevier.com/locate/clinbiomech

Biomechanical comparison between three intramedullary nails and percutaneous compression plate in stable and unstable trochanteric fractures☆

Luigi La Barbera, Ph.D. [a,*], Atsuki Tanaka, M.D. [a,b], Francesca Berti, Ph.D. [a], Guido Antonini, M.D. [c], Tomaso Villa, Ph.D. [a]

[a] LaBS, Department of Chemistry, Materials and Chemical Engineering "Giulio Natta", Politecnico di Milano, Italy
[b] Department of Orthopaedic Surgery Kobe University Graduate School of Medicine, Kobe, Hyogo, Japan.
[c] Department of Orthopedics and Traumatology, San Carlo Borromeo Hospital, Italy

ARTICLE INFO

Keywords:
Femur
Fracture
Intramedullary nailm extramedullary plate
AO/OTA classification

ABSTRACT

Background: The best surgical treatment of trochanteric fractures remains controversial and biomechanical literature lacks a comprehensive study. The study compares the behavior of fixation implants for the treatment trochanteric fractures, namely: intramedullary gamma nail, proximal femoral nail, veronail, and extramedullary percutaneous compression plate.

Methods: The implants were virtually inserted into 3D femur digital twins characterized by stable and unstable trochanteric fractures. Loadings simulated walking condition without and with crutches, respectively, for stable and unstable fractures. Stresses below the yield point quantified implant safety. Constructs' stiffness, principal strains, and the load-sharing on the fracture rims demonstrated the biomechanical advantages of fixation implant in restoring a physiological condition by comparison with the intact femur.

Findings: All implants are safe. Extramedullary plate and proximal femoral nail allowed to better recover the stiffness of the intact femur in the unstable fracture model, and the load acting along the fracture decreased respectively between 17 % and 44 % compared to stable fracture model. The minimum and maximum strain distribution was qualitatively similar for all devices, with extramedullary plate and gamma nail showing strains in the posteromedial area getting closer to the intact condition in stable fracture model. The compressive strains in the unstable fracture model treated with extramedullary plate were closer to the intact condition.

Interpretation: All investigated devices could be safely used for stable and unstable intertrochanteric fractures. The extramedullary plate may present some biomechanical advantage with unstable fractures.

1. Introduction

Trochanteric fractures are among the most common injuries in Europe with about 40–50 % of all proximal femoral fractures (Saul et al., 2019; Selim et al., 2021). A sideway fall is often the main cause, often resulting in different fracture patterns. According to standard classification, the stable trochanteric injury with two fragments is labelled as AO/OTA 31-A1, while AO/OTA 31–A2 refers to an unstable multi-fragmentary pertrochanteric fracture (Meinberg et al., 2018). Both fractures can be safely treated by a variety of internal fixation implants either including intramedullary nails and extramedullary plates, but the debate on the best option is still controversial (Bhandari and Swiontkowski, 2017).

Several authors analyzed specific fixation implant for the treatment of stable and unstable trochanteric fractures based on prospective/retrospective clinical (i.e. in vivo) studies and meta-analyses (Crespo et al., 2012; Crespo et al., 2016; Giancola et al., 2008; Kouzelis et al., 2014; Lavini et al., 2008; Marks et al., 2021; Selim et al., 2021; Shen et al., 2016; Warren et al., 2020) (Tables 1a), and biomechanical studies, either experimental (i.e. in vitro) and/or computational (i.e. in silico)

☆ This article is part of a Special issue entitled: 'Methods in Orthopaedic Biomechanics' published in Clinical Biomechanics.

* Corresponding author at: Laboratory of Biological Structure Mechanics, Department of Chemistry, Materials and Chemical Engineering "Giulio Natta", Politecnico di Milano, Piazza Leonardo da Vinci 32, 20133 Milano, Italy.
E-mail address: luigi.labarbera@polimi.it (L. La Barbera).

https://doi.org/10.1016/j.clinbiomech.2025.106507
Received 31 July 2024; Received in revised form 31 January 2025; Accepted 26 March 2025
Available online 27 March 2025

(Ding et al., 2022a; Ding et al., 2022b; Eberle et al., 2010; Goffin et al., 2014; Gotfried et al., 2002; Helwig et al., 2009; Knobe et al., 2015; Kuzyk et al., 2012; Li et al., 2019; Li et al., 2023; Lorkowski and Pokorski, 2022; Luo et al., 2013; Oken OF et al., 2011; Quental et al., 2021; Ropars et al., 2008; Taheri et al., 2011; Weiser et al., 2015; Yang et al., 2023) (Tables 1b). Most of them focused separately on one or few intra-medullary nails, such as Gamma Nail (GN), Gamma3 Nail (G3N) and Proximal Femur Nail-Antirotation (PFNA), or on extra-medullary

Table 1a
Clinical literature review including intra- and extra-medullary fixation implants for the treatment of stable / unstable trochanteric fractures.

Clinical literature review															
Author, year	Fracture model	Study design		Fixation implants											
				Intra-medullary							Extra-medullary				
		in vivo retrosp.	in vivo prosp.	GN	G3N	PFN	PFNA	Vernoail	Other		PCCP	DHS	SHS	Other	Main findings
Selim et al., 2021	AO/OTA 31-A1, 31-A2, 31-A3	✓							CMN, TSP			✓			CMN and DHS with a trochanteric stabilisation plate are effective and safe for unstable per-trochanteric fractures
Marks et al., 2021	–	✓							CMN				✓		CMN may be better than SHS in terms of QoL and hospitalization rate for geriatric patients with trochanteric femur fractures; mortality and revision rate are comparable.
Warren et al., 2020	–	✓							CMN				✓		SHS had significantly lower minor complications, but comparable major complications, discharge disposition, readmission and reoperation, length of hospital stay, and operative time vs. CMN.
Crespo et al., 2016	AO/OTA 31-A1, 31-A2	✓									✓				PCCP may be the implant of choice for AO/OTA 31.A1-A2 fracture with a complications rate of 4 % of patients (cut-out <3 %, pseudarthrosis/implant breakage <1 %).
Shen et al., 2016	–	✓		✓	✓		✓		TSRN		✓				PCCP had lower blood transfusion, hospital stay, and incidence of implant-related complications vs. intra-medullary nails (GN, GN3, PFNA, TSRN).
Kouzelis et al., 2014	AO/OTA 31-A1, 31-A2, 31-A3		✓					✓							Veronail was safe and effective for AO 31-A1, 31-A2, and 31-A3 fractures.
Crespo et al., 2012	AO/OTA 31-A1, 31-A2	✓		✓							✓				PCCP had lower overall economical cost and blood transfusion for comparable/ lower surgery-related complications.
Giancola et al., 2008	AO/OTA 31-A1, 31-A2	✓	✓	✓							✓				PCCP had lower blood loss, significantly lower transfusion need, fewer implant-related complications, lower surgical costs, but comparable healing and surgical time vs. GN.
Lavini et al., 2008	AO/OTA 31-A1, 31-A2, 31-A3		✓					✓							Veronail was effective and safe, it had satisfactory outcome in terms of healing, recovery of pain-free walking ability and low incidence of complications. Two converging locked cephalic screws proved a stable fixation in 31.A2 femoral fractures, similarly with traditional parallel sliding screws.

Intra-medullary fixation implants GN: Gamma nail. GN3: Gamma nail3. PFN: Proximal femoral nail. PFNA: Proximal femoral nail-antirotation. TSRN: Trigen short reconstruction nail. ITN: Intertan nail. CMN: Cephalomedullary nail. TSP: Trochanteric stabilisation plate. MSN: Medial sustainable nail. TSFP: triangle support fixation plate. TSIN: Triangular support intramedullary nail. G1N: Gliding nail. TPF: Targon-PF.
Extra-medullary fixation implants CCP: Percutaneous compression plating. DCS: Dynamic condylar screw. DHS: Dynamic hip screw. MAP: Modified anatomic plate. MISS: Minimally invasive screw system. SHS: Sliding hip screws. P-FLCP: proximal femoral locking compression plate.

plates, focusing extensively on Dynamic Hip Screws (DHS) and Percutaneous Compression Plates (PCCP).

Few studies directly compared modern intra- and extramedullary implants (Tables 1a,b). According to Weiser et al., in the unstable fracture model the failure load of the intramedullary nail was higher than that of an extramedullary dynamic plating system (Weiser et al., 2015). Selim et al. investigated on a clinical meta-analysis by using a cephalo-medullary nailing for the treatment of unstable fracture was associated with lower revision rates than by using a dynamic plating system (Selim et al., 2021). On the other hand, extramedullary plates have been shown to reduce postoperative blood transfusion (Warren et al., 2020), which is a desirable advantage to reduce the risk of complication. Although extramedullary plates have the disadvantage of a longer lever arm between a lag screw and plate than nails, recently many types of extramedullary devices have been developed to improve this disadvantage and clinical results. However, in most of these studies comparing extramedullary and intramedullary implants, only dynamic hip screw (DHS) was used as the extramedullary implant (Marks et al., 2021; Weiser et al., 2015). Therefore, which implants are suitable for the treatment of unstable fracture remains controversial.

Among the extramedullary fixation implants, PCCP allows minimally invasive surgery by means of two small percutaneous portals and small diameter drilling, thus reducing intraoperative bleeding (Gotfried et al., 2002; Shen et al., 2016). PCCP is also theoretically superior to the DHS as regards the rotational stability because of two dynamic cephalic screws (Giancola et al., 2008). Previous clinical studies showed that the PCCP decreased blood loss, blood transfusion, implant-related complications, surgery-related costs and comparable or lower hospital stay and surgery time compared to other intramedullary nails such as GN, G3N, PFNA (Crespo et al., 2012; Giancola et al., 2008; Lavini et al., 2008; Shen et al., 2016).

Among the intramedullary fixation implants, the Veronail is a relatively new nail for the treatment of trochanteric fracture. This has two cephalic screws available with both parallel and convergent configuration (Lavini et al., 2008). Kouzelis et al. performed a prospective study on the Veronail system in 60 patients and found stability of the device and proper operative time in both stable and unstable fractures without serious intraoperative complications. Therefore, this device would be an additional viable option for the treatment of trochanteric fractures (Kouzelis et al., 2014).

To the best of our knowledge, only few studies compared the biomechanical behavior of extramedullary fixation devices like the PCCP with other intramedullary implants using in vitro methodologies (Knobe et al., 2015; Krischak et al., 2007; Ropars et al., 2008), while no study has ever compared the PCCP and the Veronail from a biomechanical point of view by using in silico finite element (FE) analysis.

Therefore, the aim of the present computational study is to compare the biomechanical behavior of four commercial implants used to stabilize intertrochanteric fractures of the proximal femur: the intramedullary Gamma3 Nail (G3N, Stryker, Schoenkirchen, Germany), Proximal femoral nail (PFN, Synthes, Oberdorf, Switzerland), Veronail (Orthofix, Bussolengo, Italy) and the extramedullary percutaneous compression plate (PCCP, Orthofix, Bussolengo, Italy). The stresses on the devices as well as the load and strains on the fractured rims were calculated and analyzed discussing the differences between the devices in treating different types of the fracture (AO/OTA 31–A1 and AO/OTA 31–A2) and focusing, in particular, on the fixation types (intramedullary vs. extramedullary). To demonstrate the biomechanical advantage of each fixation implant in restoring a physiological condition, the intact model was assumed as a reference.

2. Methods

2.1. Intact femur model

The model of a left synthetic third generation femur (Sawbones, Pacific Research Laboratories Inc.), downloaded from the VPH NOE database (Virtual Physiological Human Network of Excellence, www.vph-noe.eu), was used. The geometry of this model was scaled to 95 % in order to obtain a size comparable with the femurs used in the validation study found in literature (Cristofolini et al., 2009).

The intact femur was imported in Abaqus Standard 2022 (Dassault Systèmes, SIMULIA Corp., RI, USA), where the distal extremity, corresponding to 40 % of the length, was resected with respect to horizontal plane. To represent an osteoporotic femur, homogeneous, isotropic, and linear elastic material properties were assigned to the femur (Young modulus E = 12.4GPa and 77 MPa for the cortical and trabecular bone, respectively, and a Poisson's ratio $\nu = 0.3$) (Goffin et al., 2014; Taheri et al., 2011).

2.2. Fractured femur models

Two fractured scenarios were reproduced, according to the AO/OTA Müller classification (Meinberg et al., 2018).

As regards AO 31–A1 (simple trochanteric fracture), the femur was cut through the small trochanter using a plane tilted of 43° with respect to the horizontal surface, so that the lateral femoral wall <20.5 mm (Goffin et al., 2014). As regards AO 31–A2 (multifragmentary pertrochanteric fracture), the lesser trochanter was also resected using two tilted planes (inclination of −25° and − 30° with respect to the horizontal and vertical directions, respectively) (Fig. 1).

2.3. Fixation implants

Moreover, the CAD models of three intramedullary nails (G3N, PFN and Veronail) and one extramedullary plate (PCCP) were reverse engineered using a digital caliper and drawn in Creo Parametric (Ver. 2.0, Parametric Technology Corporation). Each implant was virtually inserted in the femur under the supervision of a senior orthopaedic surgeon (G.A.) participating in the study (Fig. 1). A gap was kept in-between the PCCP and the femur. Linear elastic material properties typical of Ti6Al4V alloy were assigned to the nails, while those of stainless steel to the plate (Goffin et al., 2014; Taheri et al., 2011), as summarized in Table 2.

2.4. Meshing and contact conditions

A linear tetrahedral mesh (C3D4) was adopted, refining the element size on the fractured surfaces and the contact areas. A mesh convergence analysis on each model ensured that, the stresses on the fractured surface and at the interface between the devices and the screws varied less than 5 % upon subsequent mesh refinement steps. The average dimension of the elements resulted 0.3 mm at the interface between the bone and the devices, 0.5 mm on the fractured surface and between 0.7 mm and 2 mm on the rest of the models. Therefore, the total number of elements and nodes is listed in Table 2. A surface-to-surface contact was used at the bone-devices interface. The friction coefficients among different parts are reported in Table 3 (Eberle et al., 2010; Hsu et al., 2007; Sowmianarayanan et al., 2008).

2.5. Loading conditions

In case of 31–A1 fracture, a force of 1866 N was applied on the femoral head (Eberle et al., 2010; Goffin et al., 2014), representing the maximum load acting on the hip joint during walking for an 80 kg subject (Bergmann et al., 2001). For 31–A2 fracture the load was reduced to 1088 N to reproduce walking with crutches, as measured after surgery during rehabilitation exercises (Damm et al., 2013). The force vector was oriented both on the frontal (13° from the axis of the femoral shaft laterally) and on the sagittal plane (8° posteriorly) (Eberle et al., 2010). In both cases, the distal part of the femur was fully constrained.

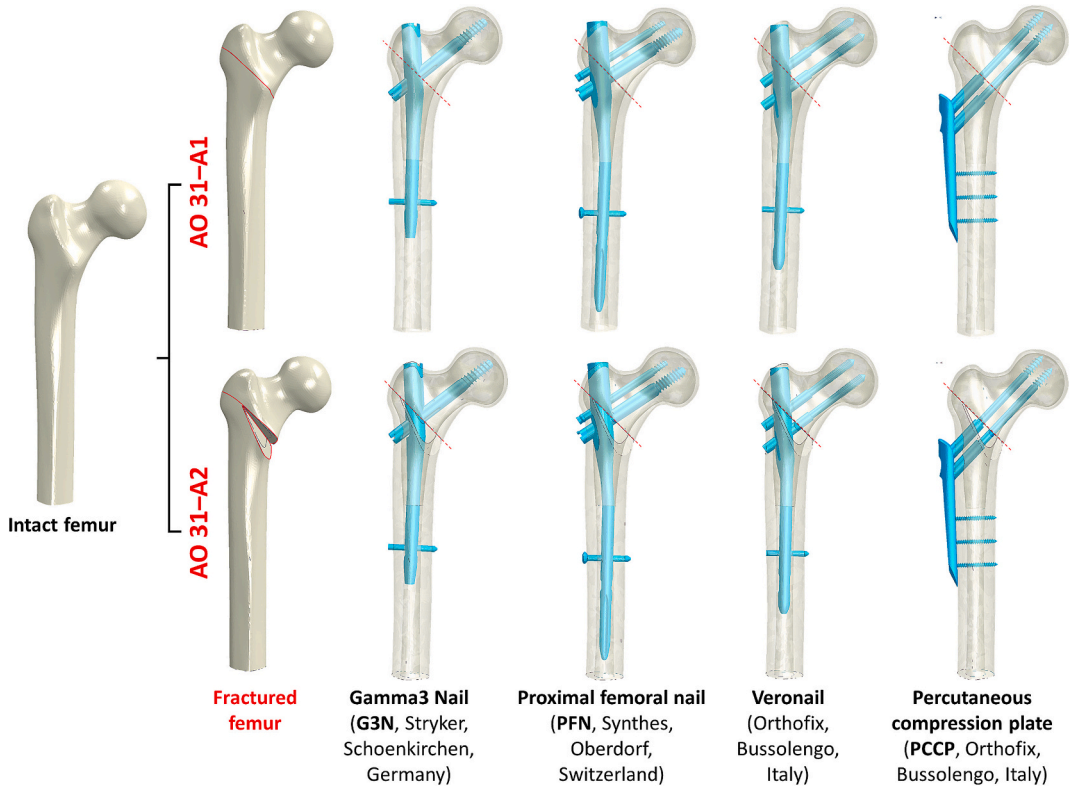

Fig. 1. Intact femur and fractured models. The 31–A1 fracture was obtained cutting the femur through the small trochanter, with a plane tilted of 43° with respect to the horizontal. The 31–A2 fracture was created removing the small trochanter with two planes (tilted of −25° and − 30° with respect to the horizontal and vertical directions, respectively). The four implants (G3N, PFN, Veronail, PCCP) were virtually inserted in the fractured models.

2.6. Data analysis

To determine whether all the fixation implants can be safely used, the von Mises stresses in the devices were calculated and compared to the static yield stress of the material (880 MPa for titanium alloys and 792 MPa for the stainless steel) (Heiney et al., 2008).

The overall stiffness of each instrumented femur, calculated dividing the maximum applied force by the vertical displacement achieved, provided a first indication on the primary stability, depending on the fracture type (Ropars et al., 2008), as well as the capability of each implant in restoring a physiological stiffness (i.e. comparable to the intact femur).

The overall load-sharing across the fracture rims was calculated based on nodal forces (NFORC), projected along the normal axis to quantify the actual mechanical stimulus promoting bone healing, and compared to each intact model.

More locally, the maximum (tensile) and minimum (compressive) principal strains both on the surrounding bone and on the fracture rims were calculated, compared to the intact femur and the static yield strain typical of bone: tensile and compressive yield strains were, respectively, 0.73 % and − 1.12 % for the cortical (Verhulp et al., 2008), and 1.74 % and − 2 % for the trabecular bone (Aleixo et al., 2013).

To demonstrate the biomechanical advantage of each fixation implant in restoring a physiological condition, the intact model was assumed as a reference both for global (i.e. stiffness), and for local (i.e. principal strains) quantities.

3. Results

3.1. Implant stresses

The maximum von Mises stresses were found at the interface between the nail/plate and the cephalic screw or between the screw and the support guide (Fig. 2, Table 4). The highest value was found in the G3N model (31–A1: 246 MPa; 31–A2: 285 MPa). As expected, von Mises stresses in 31–A2 was slightly higher than that in 31–A1, and both were always below the yield strengths of the materials.

3.2. Stiffness and load-sharing on the fracture rim

As concern the treatment of 31–A1 fracture, all the devices produced a stiffening of the fractured femur with respect to the intact femur model. The overall stiffness increased about 16 % by using the intramedullary devices, while it increased up to 25 % for the PCCP (Table 4). The load transmitted across the fracture rim decreased about 15 % with respect to the intact femur both for G3N and PCCP, while it kept almost the same for PFN and Veronail (Table 4).

As concern the treatment of 31–A2 fracture, only the PCCP and PFN allowed to recover the stiffness of the intact femur, while the other intramedullary devices (G3N and Veronail) demonstrated an average decrease beyond 5 % (Table 4). Regarding the load acting on the fractured surface, it could be noted that with 31–A2 fracture in the model with nails or plate the load acting along the fracture decreased between 17 % and 44 % with respect to 31–A1 (Table 4).

3.3. Bone strains

The local strain distribution was similar for different devices both in terms of compressive and tensile principal strain values (Figs. 3 and 4). As expected, the values were much higher for 31–A2 fracture than for 31–A1, although the applied load was lower. Considering the strain in the posteromedial area of the fracture surface (Table 4), the G3N and PCCP were able to make it closer to that of the intact femur for AO 31–A1 fracture model; while the strains reached with the PCCP was 15 % higher than the G3N for AO 31–A2 fracture. The principal strains were below the yield point in all cases.

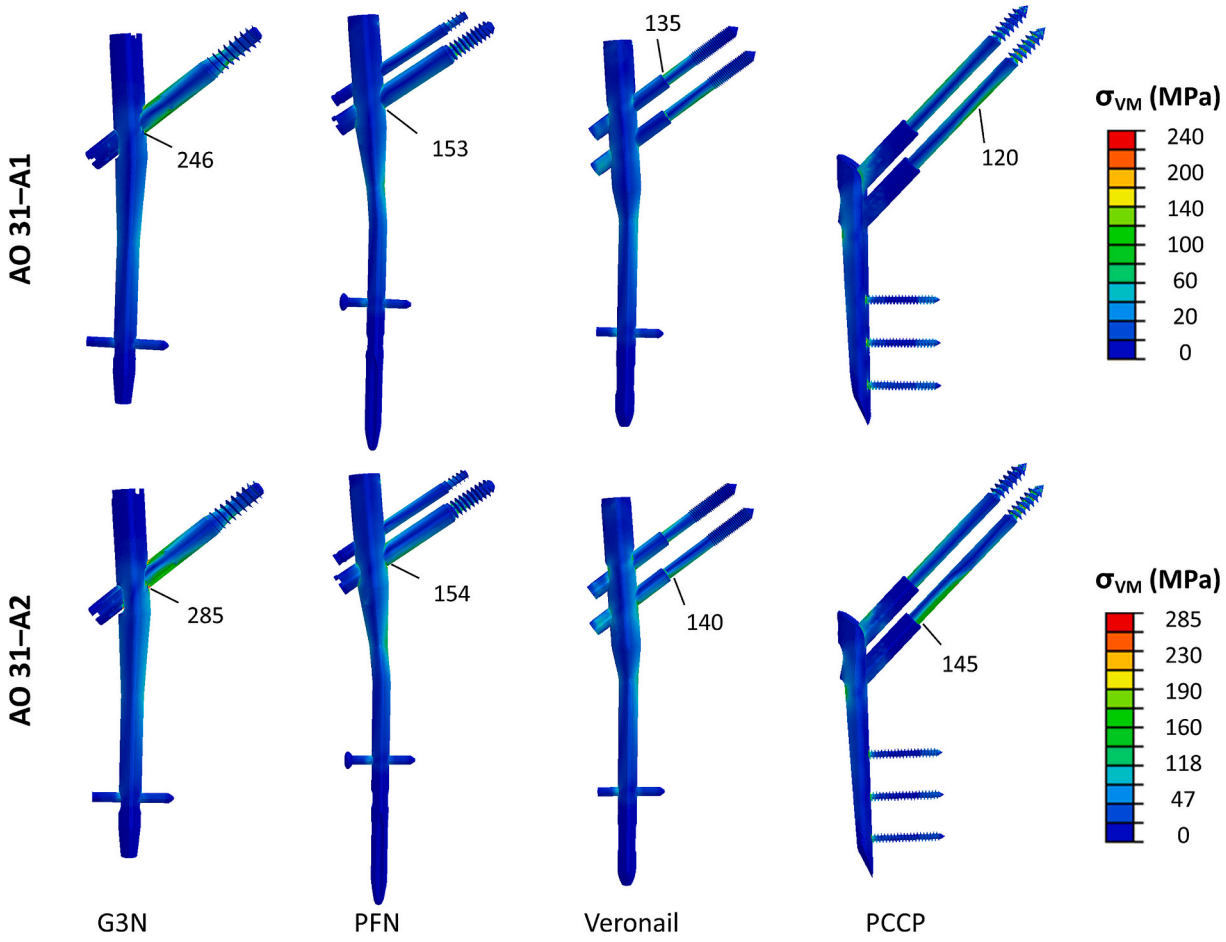

Fig. 2. The von Mises stresses of four implants (G3N, PFN, Veronail, and PCCP). The load on 31–A1 fracture model was 1866 N (Cristofolini et al., 2009; Taheri et al., 2011), and the load on 31–A2 fracture model was 1088 N (Bergmann et al., 2001). Please, refer to the online version of the paper to appreciate the color maps.

4. Discussion

Since trochanteric fractures have a high incidence in the elderly population, the number of patients is expected to continuously increase in Europe (Bhandari and Swiontkowski, 2017; Saul et al., 2019; Weiser et al., 2015). Although various innovative implants are continuously designed and updated, post-operative complications are still very common. The goal of the present study was to compare the biomechanical behavior of widely used implants for the treatment of pertrochanteric fractures never compared so far: the intramedullary G3N, PFN, Veronail, and the extramedullary PCCP. While the GN and PFN have been widely used since 1990s, on the other hand the Veronail and PCCP were relative newer devices which have developed in the 2000s (Gotfried et al., 2002; Lavini et al., 2008).

Several prospective/retrospective clinical studies and meta-analyses (Table 1a) (Crespo et al., 2012; Crespo et al., 2016; Giancola et al., 2008; Kouzelis et al., 2014; Lavini et al., 2008; Marks et al., 2021; Selim et al., 2021; Shen et al., 2016; Warren et al., 2020), and biomechanical experimental and/or computational studies (Table 1.b) (Ding et al., 2022a; Ding et al., 2022b; Eberle et al., 2010; Goffin et al., 2014; Gotfried et al., 2002; Helwig et al., 2009; Knobe et al., 2015; Kuzyk et al., 2012; Li et al., 2019; Li et al., 2023; Lorkowski and Pokorski, 2022; Luo et al., 2013; Oken OF et al., 2011; Quental et al., 2021; Ropars et al., 2008; Taheri et al., 2011; Weiser et al., 2015; Yang et al., 2023) analyzed specific fixation implant for the treatment of stable and unstable trochanteric fractures with controversial results, but very few of them directly compared intra- and extra-medullary implants.

The present biomechanical study presents an in silico computational (FE) approach to virtually simulate primary stabilisation of the fractured femur and obtaining unique quantitative insights on their biomechanical behavior, not measurable during experimental tests, nor during clinical studies. To the authors' knowledge this is the first study comparing all these devices, especially the PCCP and Veronail which received very little attention in the past literature (Gotfried et al., 2002; Knobe et al., 2015; Ropars et al., 2008).

Some researchers investigated the fixation of trochanteric fracture by using finite element method (Table 1.b). Helwig et al. (Helwig et al., 2009) investigated 31–A2 fracture type and the use of four different nails (PFN-A, GN, G1N, TPF), but their study only studied implant positioning and its influence on fracture healing. Oken et al. (Oken OF et al., 2011) compared the use of a nail and a plate following 31–A1 fracture, with a mixed in vitro and in silico approach; however, they considered a different load case and calculated the stress on the fractured surface without providing insights on primary stability (i.e. stiffness). Ding et al. (Ding et al., 2022a; Ding et al., 2022b) only compared intramedullary nail techniques for the fixation of stable and unstable intertrochanteric fractures using a rather unrealistic low load of 600 N, but reporting about the displacement of the fracture surface and a comparison with in vitro experiments. Goffin et al. (Goffin et al., 2014) compared the use of a Gamma Nail and a SHS plate, focusing only on the safety of the implants and analyzing the bone strains only in the femoral neck around the cephalic screw (potentially involved in cut-out).

In the present study we observed that the most stressed regions of each fixation implant were located at the interface between the nail and the screws or between the screw and the support guide (Fig. 2, Table 4), in nice agreement with the published literature (Ding et al., 2022b;

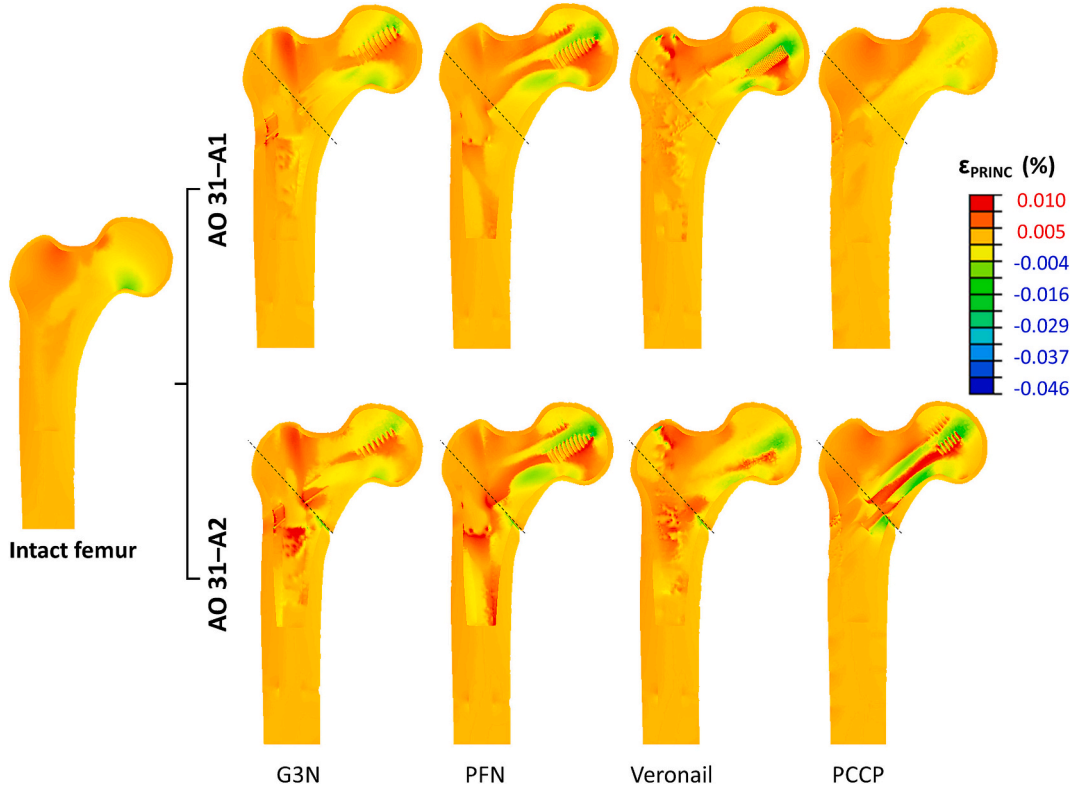

Fig. 3. Principal strains – Coronal views of the intact femur and fractured models (31–A1and 31–A2) with each fixation implant (G3N, PFN, Veronail, PCCP). Please, refer to the online version of the paper to appreciate the color maps.

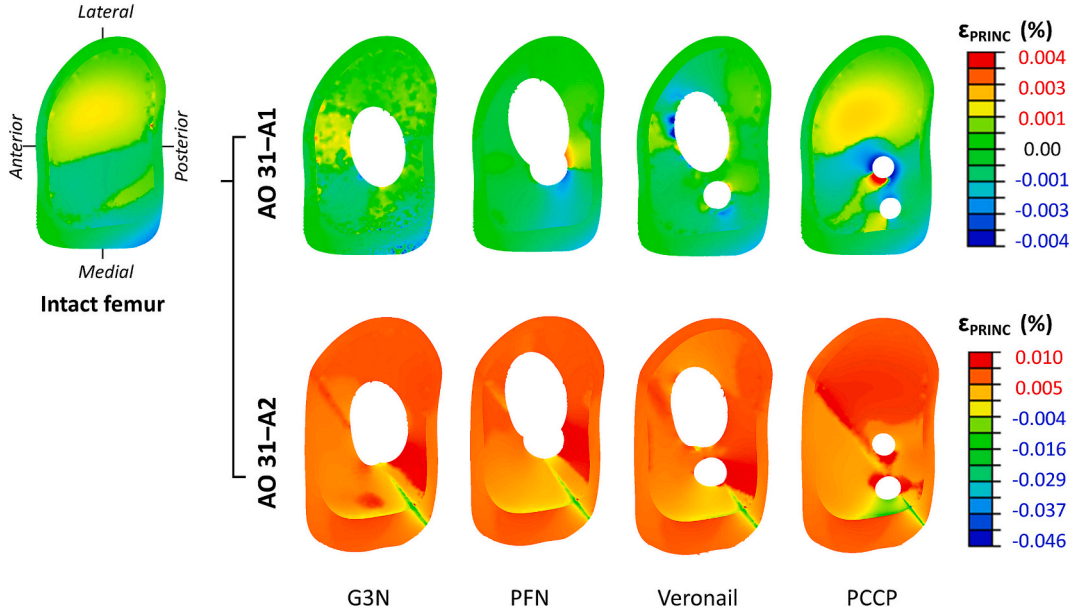

Fig. 4. Principal strains – Normal views of the intact femur and the fractured models (AO 31–A1 and 31–A2) with each implant (G3N, PFN, Veronail, PCCP). Please, refer to the online version of the paper to appreciate the color maps.

Goffin et al., 2014; Luo et al., 2013). Despite the critical loading condition reproducing the peak loads met during normal walking and walking with crutches, respectively in stable (AO 31–A1) and unstable (AO 31–A2) fractured models, all the fixation implants proved to be safe, as the implant stresses were always below the yield point. As expected, we observed that, despite the applied load was about 40 % lower for 31–A2 vs. 31–A1 fracture models (1088 vs. 1866 N), the implant stresses were similar for stable and unstable fracture models with the same fixation implant, supporting that, as expected, unstable fractures (AO 31–A2) are a more critical condition compared to stable fractures (AO 31–A1).

As for the 31–A2 fracture model the maximum von Mises stresses (Table 4) of two cephalic screw implants (PFN and Veronail) were about 50 % lower than that of the one cephalic screw implant (G3N); our study

Table 1.b
Biomechanical literature review including intra- and extra-medullary fixation implants for the treatment of stable / unstable trochanteric fractures.

Biomechanical literature review															
Author, year	Fracture model	Study design		Fixation implants											
				Intra-medullary							Extra-medullary				
		in silico	in vitro/ ex vivo	GN	G3N	PFN	PFNA	Vernoail	Other		PCCP	DHS	SHS	Other	Main findings
Present study	**AO/OTA 31-A1, 31-A2**	✓			✓	✓		✓			✓				
Yang et al., 2023	AO/OTA 31-A2	✓					✓								Inferior-posterior placement of the helical blade provided higher stiffness and lower bone strains and implant stresses.
Li et al., 2023	AO/OTA 31-A2	✓					✓					✓		P-FLCP	PFNA could provide better stability/stiffness and undergo lower stresses than DHS and P-FLCP. Buttress strength was proportional to the thickness of the femoral lateral wall.
Lorkowski and Pokorski, 2022	AO/OTA 31-A1, A2, A3			✓								✓			Comparable bone stresses for GNF and DHS; lower stresses for A1 than A3 fractures. GNF had higher implant stresses vs. DHS.
Ding et al., 2022a	Evans type I, IV	✓	✓						TSFP			✓			TSFP had higher stability, lower bone stresses, reduced implant stresses vs. DHS.
Ding et al., 2022b	Evans type I, IV	✓	✓	✓			✓		TSIN						TSIN was better than GN and PFNA in terms of stress distribution and construct stability.
Quental et al., 2021	AO/OTA 31-A2	✓					✓								Inferior and deep placement of the lag screw was the best position to reduce cut-out risk.
Li et al., 2019	AO/OTA 31-A2.3	✓	✓				✓							MSN	MSN construct might exhibit a better biomechanical performance than PFNA in reducing displacement and anti-varus in fracture type of AO/OTA 31-A2.3.
Weiser et al., 2015	AO/OTA 31-A2.3		✓						ITN			✓			DHS and ITN had comparable stiffness and survival during cyclic testing. ITN had a significantly higher failure load.
Knobe et al., 2015	AO/OTA 31-A2.2		✓						ITN		✓				ITN was stronger than PCCP in terms of number of cycles achieved under sequential load increases for unstable fractures; stiffness was comparable, both had a high rotational stability and lateral wall support.
Goffin et al., 2014	AO/OTA 31-A2 or Evans types IV, V	✓		✓									✓		Evans' type V fractures stabilized with a GN and Evans' types IV and with SHS exposed the osteoporotic cancellous bone around the lag crew to yielding and cut-out.
Luo et al., 2013	AO/OTA 31-A2.2		✓									✓			DHS blade was superior in resisting vertical or rotational displacement compared with conventional DHS threaded screws.
Kuzyk et al., 2012	Unstable peri-trochanteric		✓		✓										Stiffness (i.e. primary stability) increased with cephalic screws positioned along the inferior margin of the femoral neck/head.

(*continued on next page*)

Table 1.b (*continued*)

Biomechanical literature review															
Author, year	Fracture model	Study design		Fixation implants											
				Intra-medullary							Extra-medullary				
		in silico	in vitro/ ex vivo	GN	G3N	PFN	PFNA	Vernoail	Other		PCCP	DHS	SHS	Other	Main findings
Taheri et al., 2011	–	✓										✓			Stress-shielding minimized by Ti-alloys vs. stainless steel; bone stresses during stance were higher on implanted femur vs. intact.
Oken OF et al., 2011	Inter-trochanteric	✓	✓			✓						✓		MAP	MAP generated optimal loads at both the fracture site and the proximal femur. PFN and MAP demonstrated similar biomechanical performance.
Eberle et al., 2010	AO/OTA 31-A3.1, 31-A3.3	✓		✓											A reinforced GN was beneficial in subtrochanteric fractures to reduce stresses without increasing stress-shielding.
Helwig et al., 2009	Trochanteric	✓		✓			✓			G1N, TPF					PFN-A, Gamma-Nail and GIN promote fracture healing when positioned caudally. TPF advantageous in caudal position.
Ropars et al., 2008	–		✓								✓			MISS	PCCP had good/comparable clinical outcomes and reduced risk of co-morbidities with unstable trochanteric fractures without increased risk of mechanical failure.
Gotfried et al., 2002	Inter-trochanteric		✓								✓				PCCP provided adequate bending stiffness and torsional stability; sliding allows controlled fracture impaction.

Table 2
Materials, material properties (E: elastic modulus, ν: Poisson ratio) and total number of elements (nodes) for each model.

Fracture type	Model	Materials	Material properties	Elements (Nodes)
31–A1	G3N	Ti6Al4V	Lin. elastic (E = 113.8 GPa, ν = 0.34)	278,493 (1,295,251)
	PFN	Ti6Al4V	Lin. elastic (E = 113.8 GPa, ν = 0.34)	367,168 (1,725,151)
	Veronail	Ti6Al4V	Lin. elastic (E = 113.8 GPa, ν = 0.34)	349,317 (1,604,668)
	PCCP	Stainless-steel	Lin. elastic (E = 195 GPa, ν = 0.3)	353,020 (1,633,054)
31–A2	G3N	Ti6Al4V	Lin. elastic (E = 113.8 GPa, ν = 0.34)	275,849 (1,282,490)
	PFN	Ti6Al4V	Lin. elastic (E = 113.8 GPa, ν = 0.34)	370,144 (1,739,142)
	Veronail	Ti6Al4V	Lin. elastic (E = 113.8 GPa, ν = 0.34)	352,061 (1,619,893)
	PCCP	Stainless-steel	Lin. elastic (E = 195 GPa, ν = 0.3)	355,126 (1,644,996)

Table 3
Friction coefficients assumed to describe the interaction among different model components.

Components	Friction coefficient	Reference
Bone/Bone	0.46	Eberle et al. (Helwig et al., 2009)
Ti6Al4V/ Ti6Al4V	0.23	Eberle et al. (Helwig et al., 2009)
Bone/Ti6Al4V	0.30	Eberle et al. (Helwig et al., 2009)
Steel/Steel	0.20	Sowmianarayanan et al. (Ropars et al., 2008)
Bone/Steel	0.42	Hsu et al. (Gotfried et al., 2002)

seems to indicate that the number of cephalic screws plays a more relevant role in reducing the maximum implant stresses of unstable fracture, rather than the extramedullary or intramedullary approach itself. Knobe et al. (Knobe et al., 2015) experimentally investigated the behavior of the PCCP for the unstable trochanteric fracture in vitro, and they found that the middle part of the inferior screw supports the bending, providing a confirmation about the position of the maximum von Mises stress found in our numerical study. Moreover, in their experiments the PCCP survived the load assumed in the daily life (Knobe et al., 2015), thus confirming the mechanical reliability of the device in accordance with our result, which also reported that the stresses on the PCCP device were safe.

Regarding primary stability (Table 4), the present study agrees with other studies (Ding et al., 2022a; Ding et al., 2022b) reporting stiffness values in a similar range for stable intertrochanteric fractures. Moreover, we found that the stiffness of the implanted femurs is obviously related to the material (i.e. devices in stainless steel were stiffer than those in Ti6Al4V), but also to the screw positioning and, to the number of screws. Therefore, among the Ti6Al4V nails, GN resulted the intramedullary device with the lower stiffness, having a single cephalic screw centered in the femoral neck, compared to PFN and Veronail, which had two cephalic screws. The PCCP instead, is the stiffest device being built

Table 4
Implant stresses, overall stiffness, normal compressive load transferred across the racture rim and the minimum principal strain in the postero-medial region of the fracture surface for each fixation implant and fracture model. Percentage differences compared to yield or the intact condition are reported.

Fracture model	Fixation implant	Implant stresses			Stiffness			Fracture rim					
								Normal load			Minimum principal strain		
		(MPa)	*(% vs. yield)*	*(% vs. 31-A1)*	(N/mm)	*(% vs. yield)*	*(% vs. 31-A1)*	(N)	*(% vs. yield)*	*(% vs. 31-A1)*	(N)	*(% vs. yield)*	*(% vs. 31-A1)*
AO/OTA 31–A1	Intact	–	–	–	2475	–	–	626		–	−0.234	–	–
	G3N	246	*−72 %*	–	2801	*+13 %*	–	532	*−15 %*	–	−0.201	*–14 %*	–
	PFN	153	*−83 %*	–	2854	*+15 %*	–	649	*+4 %*	–	−0.188	*–20 %*	–
	Veronail	135	*−85 %*	–	2984	*+21 %*	–	594	*–5 %*	–	−0.194	*–17 %*	–
	PCCP	120	*−85 %*	–	3090	*+25 %*	–	530	*−15 %*	–	−0.203	*–13 %*	–
AO/OTA 31–A2	G3N	285	*−68 %*	*+16 %*	2247	*–9 %*	*−20 %*	439	*−30 %*	*−17 %*	−0.997	*+326 %*	*+396 %*
	PFN	154	*−83 %*	*+1 %*	2441	*–1 %*	*−14 %*	489	*−22 %*	*−25 %*	−0.992	*+324 %*	*+428 %*
	Veronail	140	*−84 %*	*+4 %*	2351	*–5 %*	*−21 %*	471	*−25 %*	*−21 %*	−0.936	*+300 %*	*+382 %*
	PCCP	145	*−82 %*	*+21 %*	2491	*+1 %*	*−19 %*	296	*−53 %*	*−44 %*	−0.842	*+260 %*	*+315 %*

in stainless steel and having two cephalic screws. According to Kuzyk et al. (Kuzyk et al., 2012), also the position of the cephalic screw plays and important mechanical role in unstable trochanteric fractures, as its positioning along the inferior margin of the femoral neck and head – which is the portion undergoing compression during standing and the peak load of the stance phase during walking – increases the stiffness of the fractured femur treated with G3N. In our study, the PCCP has two cephalic screws, with one of them very close to the cortical layer in the inferior part of the femoral head, therefore, the combined effect of a stiffer material and double cephalic screws may justify the higher stiffness of PCCP compared with other intramedullary devices.

The principal strains maps revealed important differences among different fixation devices, due to the differences in terms of design and cephalic screw number and placement (Figs. 3 and 4, Table 4). The most critical compressive strain was always observed on the posteromedial area of the fracture rim close to the medial cortex, as also reported by Ding et al. (Ding et al., 2022a; Ding et al., 2022b): strains were relatively low for stable (31–A1) fractures, but increase of about 4.8 times with unstable (31–A2) fractures, supporting that the removal of the lesser trochanter largely affected the result. Nevertheless, the principal strains never exceeded critical values (Aleixo et al., 2013; Verhulp et al., 2008).

While past studies only compared specific fixation devices totally neglecting the physiological loading occurring in the intact condition, we believe that only a direct comparison with the intact condition would ensure a clearer interpretation of the biomechanical contributions of each implant design for the fixation of stable and unstable intertrochanteric fractures, as well as to relate global (i.e. stiffness, normal forces) and local information (i.e. strains) on the bony structures (Table 4). When considering a stable 31–A1 fracture, all fixation implants stiffened the fractured femur compared to the intact condition of about 18 % (from 13 % with G3N, up to 25 % with PCCP), thus resulting in a stress-shielding effect, where the normal compressive load on the fracture rim decreased of about 8 % (from −15 % with G3N and PCCP, up to +4 % with PFN), as reflected by a reduction of about 16 % (from −13 % with PCCP, up to −20 % with PFN) of the compressive principal strain in the posterolateral region. Despite PFN seemed to promote an effective load-sharing on the fracture rim (+4 % compared to the physiological intact condition), the principal strains were the lowest (Table 4).

Conversely, when considering an unstable 31–A2 fracture, only PCCP and PFN could restore the physiological stiffness obtained in the intact condition (within 1 %), while Veronail and G3N could not (−5 % and − 9 %, respectively). As already discussed for stable fractures, also for unstable 31-A2 fractures, a stress-shielding effect was observed with an overall reduction of 32 % of the normal compressive load on the fracture rim (from −22 % with PFN, up to −53 % with PCCP), however, the compressive principal strain in the posterolateral region significantly increased of about 300 % (from +260 % with PCCP, up to +326 % with G3N). Interestingly, another biomechanical study (Ding et al., 2022b) compared GN with PFNA, an upgrade of the PFN (included herein, with a single cephalic screw), and reported comparable results in terms of primary stability, local stresses and strains with similar devices.

The different biomechanical behavior (i.e. stiffness and strain distribution) observed for stable 31–A1 and unstable 31–A2 fracture further confirms the key biomechanical role of the lesser trochanter (absent in 31-A2 intertrochanteric fractures) in providing significant stability to the fractured femur and avoiding strain-intensification effects.

Some limitations affected the present study. Firstly, the use of homogenous and elastic materials (Ding et al., 2022a; Ding et al., 2022b; Goffin et al., 2014; Kuzyk et al., 2012), and a standardized 3D femur model (Eberle et al., 2010). Secondly bone pre-loads due to implantation were neglected and the presence of the muscles was not considered in our study and the fractures were assumed as a perfect planar cuts: these assumptions were deemed acceptable to describe an ideal condition where fracture reduction was optimal, to avoid increasing model complexity, while accounting for complex (i.e., multi-axial) loadings. Even if those aspects can be considered as far from any realistic clinical condition, these choices were made to ensure reproducibility and comparability of results, which is the base of biomechanical scientific studies. Therefore, these limitations, which are common to many past studies (Ding et al., 2022a; Ding et al., 2022b; Eberle et al., 2010; Goffin et al., 2014; Helwig et al., 2009; Kuzyk et al., 2012; Li et al., 2019; Luo et al., 2013; Oken OF et al., 2011; Taheri et al., 2011), should be considered acceptable, considering the overall comparative purposes of the current analysis, or even advantageous in highlighting specific biomechanical effects that may be hidden by several confounding effects in the clinical practice (subject-specific bone mineral density, variability in patients' sizes, weights, muscles and loading directions, heterogeneous fracture patterns, surgical strategy).

Although verification and validation are essential steps when dealing with any model, the present study adopted a pragmatic methodology to demonstrate the credibility of the adopted models. The intact femur model was previously validated by Franceschini et al. (Franceschini et al., 2020) in terms of stiffness and local strain distributions against experimental in vitro studies reproducing standing (Cristofolini et al., 2009) and sideways fall conditions (Grassi et al., 2012; Zani et al., 2012). Instead, an indirect validation with selected biomechanical in vitro and in silico study from Table 1b was briefly reported for the Fractured femur models following implantations with various fixation implants both in terms of stiffness for stable intertrochanteric fractures (Ding et al., 2022a; Ding et al., 2022b) and unstable trochanteric fractures (Kuzyk et al., 2012), and in terms of stress maps on the implants (Ding et al., 2022b; Goffin et al., 2014; Knobe et al., 2015; Luo et al., 2013).

5. Conclusion

The present biomechanical study supports that all investigated intramedullary (G3N, PFN, and Veronail) and extramedullary (PCCP) devices could be safely used for the treatment of stable and unstable intertrochanteric fractures. In particular, the extramedullary PCCP may behave similarly to other intramedullary fixation implants in case of stable AO 31–A1 fracture, while presenting some relative advantage in case of unstable AO 31–A2 fractures.

CRediT authorship contribution statement

Luigi La Barbera: Writing – review & editing, Writing – original draft, Visualization, Validation, Supervision, Software, Methodology, Investigation, Formal analysis, Data curation, Conceptualization. **Atsuki Tanaka:** Writing – original draft, Visualization, Investigation. **Francesca Berti:** Writing – review & editing, Writing – original draft, Investigation, Formal analysis, Data curation. **Guido Antonini:** Writing – review & editing, Writing – original draft, Investigation, Conceptualization. **Tomaso Villa:** Writing – review & editing, Writing – original draft, Supervision, Resources, Project administration, Investigation, Funding acquisition, Conceptualization.

Declaration of competing interest

This research was partially funded by MIUR FISR—FISR2019_03221 CECOMES.

Acknowledgments

Paolo Sfamurri is kindly acknowledged for his contribution on CAD drawings of the implants and simulations. Claudia Ottardi Ph.D. is kindly acknowledged for providing comments in the initial part of this study.

References

Aleixo, I., Vale, A.C., Lúcio, M., Amaral, P.M., Rosa, L.G., Caetano-Lopes, J., et al., 2013. A method for the evaluation of femoral head trabecular bone compressive properties. Mater. Sci. Forum 730–732, 3–8. https://doi.org/10.4028/www.scientific.net/MSF.730-732.3.

Bergmann, G., Deuretzbacher, G., Heller, M., Graichen, F., Rohlmann, A., 2001. Hip contact and gait patterns from routine activities. J. Biomech. 34, 859–871. https://doi.org/10.1016/s0021-9290(01)00040-9.

Bhandari, M., Swiontkowski, M., 2017. Management of acute hip fracture. N. Engl. J. Med. 377, 2053–2062. https://doi.org/10.1056/NEJMcp1611090.

Crespo, E., Galvez, J., Tenías, J.M., Cano, I., Crespo, R., Palacios, V., 2012. A comparative study between gamma nail and percutaneous compression plating for the treatment of intertrochanteric hip fractures. Eur. J. Trauma Emerg. Surg. 38 (4), 443–449. https://doi.org/10.1007/s00068-012-0181-2.

Crespo, E., Gómez, S., Palacios, V., Galvez, J., Tenías, J.M., Cano, I., et al., 2016. Long-term results after treatment of pertrochanteric femoral fractures with percutaneous compression plate (PCCP). Eur. J. Orthop. Surg. Traumatol. 26 (6), 613–617. https://doi.org/10.1007/s00590-016-1805-8.

Cristofolini, L., Juszczyk, M., Taddei, F., Viceconti, M., 2009. Strain distribution in the proximal human femoral metaphysis. Proc. Inst. Mech. Eng. Part H J. Eng. Med. 223 (3), 273–288. https://doi.org/10.1243/09544119JEIM497.

Damm, P., Schwachmeyer, V., Dymke, J., Bender, A., Bergmann, G., 2013. In vivo hip joint loads during three methods of walking with forearm crutches. Clin. Biomech. 28 (5), 530–535. https://doi.org/10.1016/j.clinbiomech.2012.12.003.

Ding, K., Zhu, Y., Wang, H., Li, Y., Yang, W., Cheng, X., Zhang, Y., Chen, W., Zhang, Q., 2022 May. A comparative study of novel extramedullary fixation and dynamic hip screw in the fixation of intertrochanteric fracture: a finite-element analysis. Front. Surg. 25 (9), 911141. https://doi.org/10.3389/fsurg.2022.911141.

Ding, F., Zhu, Y., Li, Y., et al., 2022b. Triangular support intramedullary nail: a new internal fixation innovation for treating intertrochanteric fracture and its finite element analysis. Injury S0020-1383 (22), 00222–00224. https://doi.org/10.1016/j.injury.2022.03.032.

Eberle, S., Gerber, C., Von Oldenburg, G., Högel, F., Augat, P., 2010. A biomechanical evaluation of orthopaedic implants for hip fractures by finite element analysis and in-vitro tests. Proc. Inst. Mech. Eng. Part H J. Eng. Med. 224 (10), 1141–1152. https://doi.org/10.1243/09544119JEIM799.

Franceschini, M., La Barbera, L., Anticonome, A., Ottardi, C., Tanaka, A., Villa, T., 2020 Dec. Hip Int. 30 (2_suppl), 86–93. https://doi.org/10.1177/1120700020971312.

Giancola, R., Antonini, G., Delle Rose, G., Crippa, C., 2008. Percutaneous compression plating versus gamma nail for the treatment of pertrochanteric hip fractures. Strateg Trauma Limb Reconstr. 3 (1), 9–14. https://doi.org/10.1007/s11751-008-0032-1.

Goffin, J.M., Pankaj, P., Simpson, A.H., 2014. A computational study on the effect of fracture intrusion distance in three- and fourpart trochanteric fractures treated with gamma nail and sliding hip screw. J. Orthop. Res. 32 (1), 39–45. https://doi.org/10.1002/jor.22469.

Gotfried, Y., Cohen, B., Rotem, A., 2002. Biomechanical evaluation of the percutaneous compression plating system for hip fractures. J. Orthop. Trauma 16, 644–650. https://doi.org/10.1097/00005131-200210000-00006.

Grassi, L., Schileo, E., Taddei, F., et al., 2012. Accuracy of finite element predictions in sideways load configurations for the proximal human femur. J. Biomech. 45, 394–399. https://doi.org/10.1016/j.jbiomech.2011.10.019.

Heiney, J., Battula, S., Njus, G., Ruble, C., Vrabec, G., 2008. Biomechanical comparison of three second-generation reconstruction nails in an unstable subtrochanteric femur fracture model. Proc. Inst. Mech. Eng. Part H J. Eng. Med. 222 (6), 959–966. https://doi.org/10.1243/09544119JEIM369.

Helwig, P., Faust, G., Hindenlang, U., Hirschmüller, A., Konstantinidis, L., Bahrs, C., et al., 2009. Finite element analysis of four different implants inserted in different positions to stabilize an idealized trochanteric femoral fracture. Injury 40 (3), 288–295. https://doi.org/10.1016/j.injury.2008.08.016.

Hsu, J.T., Chang, C.H., Huang, H.L., Zobitz, M.E., Chen, W.P., Lai, K.A., et al., 2007. The number of screws, bone quality, and friction coefficient affect acetabular cup stability. Med. Eng. Phys. 29 (10), 1089–1095. https://doi.org/10.1016/j.medengphy.2006.11.005.

Knobe, M., Gradl, G., Buecking, B., Gackstatter, S., Sönmez, T.T., Ghassemi, A., et al., 2015. Locked minimally invasive plating versus fourth generation nailing in the treatment of AO/OTA 31A2.2 fractures: a biomechanical comparison of PCCP® and Intertan nail®. Injury 46 (8), 1475–1482. https://doi.org/10.1016/j.injury.2015.05.011.

Kouzelis, A., Kravvas, A., Mylonas, S., Giannikas, D., Panagopoulos, A., 2014. Double Axis Cephalocondylic fixation of stable and unstable intertrochanteric fractures: early results in 60 cases with the Veronail system. Open Orthop. J. 8 (1), 60–68. https://doi.org/10.2174/1874325001408010060.

Krischak, G.D., Augat, P., Beck, A., Arand, M., Baier, B., Blakytny, R., et al., 2007. Biomechanical comparison of two side plate fixation techniques in an unstable intertrochanteric osteotomy model: sliding hip screw and percutaneous compression plate. Clin. Biomech. 22 (10), 1112–1118. https://doi.org/10.1016/j.clinbiomech.2007.07.016.

Kuzyk, P.R.T., Zdero, R., Shah, S., Olsen, M., Waddell, J.P., Schemitsch, E.H., 2012. Femoral head lag screw position for cephalomedullary nails: a biomechanical analysis. J. Orthop. Trauma 26 (7), 414–421. https://doi.org/10.1097/BOT.0b013e318229acca.

Lavini, F., Renzi-Brivio, L., Aulisa, R., Cherubino, F., Di Seglio, P.L., Galante, N., et al., 2008. The treatment of stable and unstable proximal femoral fractures with a new trochanteric nail: results of a multicentre study with the Veronail. Strateg Trauma Limb Reconstr. 3 (1), 15–22. https://doi.org/10.1007/s11751-008-0035-y.

Li, J., Han, L., Zhang, H., Zhao, Z., Su, X., Zhou, J., et al., 2019. Medial sustainable nail versus proximal femoral nail antirotation in treating AO/OTA 31-A2.3 fractures: finite element analysis and biomechanical evaluation. Injury 50 (3), 648–656. https://doi.org/10.1016/j.injury.2019.02.008.

Li, S., Su, Z.H., Zhu, J.M., Sun, W.J., Zhu, Y.C., Wang, J., Li, K., Ni, M., Han, S., 2023 Aug 4. The importance of the thickness of femoral lateral wall for treating intertrochanteric fractures: a finite elements analysis. Sci. Rep. 13 (1), 12679. https://doi.org/10.1038/s41598-023-39879-9.

Lorkowski, J., Pokorski, M., 2022 Mar 28. In silico finite element modeling of stress distribution in osteosynthesis after pertrochanteric fractures. Clin. Med. 11 (7), 1885. https://doi.org/10.3390/jcm11071885.

Luo, Q., Yuen, G., Lau, T.W., Yeung, K., Leung, F., 2013. A biomechanical study comparing helical blade with screw design for sliding hip fixations of unstable intertrochanteric fractures. Sci. World J., 351936 https://doi.org/10.1155/2013/351936.

Marks, L., Pass, B., Knobe, M., Volland, R., Eschbach, D., Lendemans, S., et al., 2021. Quality of life, walking ability and change of living situation after trochanteric femur fracture in geriatric patients–comparison between sliding hip screw and cephalomedullary nails from the registry for geriatric trauma. Injury 52 (7), 1793–1800. https://doi.org/10.1016/j.injury.2021.05.012.

Meinberg, E., Agel, J., Roberts, C., Karam, M., Kellam, J., 2018. Fracture and dislocation classification compendium–2018. J. Orthop. Trauma 32, S33–S44. https://doi.org/10.1097/BOT.0000000000001063.

Oken OF, Soydan, Z., Yildirim, A.O., et al., 2011. Performance of modified anatomic plates is comparable to proximal femoral nail, dynamic hip screw and anatomic plates: finite element and biomechanical testing. Injury 42, 1077–1083. https://doi.org/10.1016/j.injury.2011.03.014.

Quental, C., Vasconcelos, S., Folgado, J., Guerra-Pinto, F., 2021 Nov. Influence of the PFNA screw position on the risk of cut-out in an unstable intertrochanteric fracture: a computational analysis. Med. Eng. Phys. 97, 70–76. https://doi.org/10.1016/j.medengphy.2021.10.001.

Ropars, M., Mitton, D., Skalli, W., 2008. Minimally invasive screw plates for surgery of unstable intertrochanteric femoral fractures: a biomechanical comparative study. Clin. Biomech. 23, 1012–1017. https://doi.org/10.1016/j.clinbiomech.2008.04.018.

Saul, D., Riekenberg, J., Ammon, J.C., Hoffmann, D.B., Sehmisch, S., 2019. Hip fractures: therapy, timing, and complication Spectrum. Orthop. Surg. 11 (6), 994–1002. https://doi.org/10.1111/os.12524.

Selim, A., Ponugoti, N., Naqvi, A.Z., Magill, H., 2021. Cephalo-medullary nailing versus dynamic hip screw with trochanteric stabilisation plate for the treatment of unstable per-trochanteric hip fractures: a meta-analysis. J. Orthop. Surg. Res. 16 (1), 1–9. https://doi.org/10.1186/s13018-020-02193-5.

Shen, J., Hu, C., Yu, S., Huang, K., Xie, Z., 2016. A meta-analysis of percutenous compression plate versus intramedullary nail for treatment of intertrochanteric HIP fractures. Int. J. Surg. 29 (30), 151–158. https://doi.org/10.1016/j.ijsu.2016.03.065.

Sowmianarayanan, S., Chandrasekaran, A., Kumar, R.K., 2008. Finite element analysis of a subtrochanteric fractured femur with dynamic hip screw, dynamic condylar screw, and proximal femur nail implants - a comparative study. Proc. Inst. Mech. Eng. Part H J. Eng. Med. 222, 117–127. https://doi.org/10.1243/09544119JEIM156.

Taheri, N.S., Blicblau, A.S., Singh, M., 2011. Comparative study of two materials for dynamic hip screw during fall and gait loading: titanium alloy and stainless steel. J. Orthop. Sci. 16, 805–813. https://doi.org/10.1007/s00776-011-0145-0.

Verhulp, E., van Rietbergen, B., Huiskes, R., 2008. Load distribution in the healthy and osteoporotic human proximal femur during a fall to the side. Bone 42, 30–35. https://doi.org/10.1016/j.bone.2007.08.039.

Warren, J.A., Sundaram, K., Hampton, R., McLaughlin, J., Patterson, B., Higuera, C.A., et al., 2020. Cephalomedullary nailing versus sliding hip screws for intertrochanteric and basicervical hip fractures: a propensity-matched study of short-term outcomes in over 17,000 patients. Eur. J. Orthop. Surg. Traumatol. 30 (2), 243–250. https://doi.org/10.1007/s00590-019-02543-y.

Weiser, L., Ruppel, A.A., Nüchtern, J.V., Sellenschloh, K., Zeichen, J., Püschel, K., et al., 2015. Extra- vs. intramedullary treatment of pertrochanteric fractures: a biomechanical in vitro study comparing dynamic hip screw and intramedullary nail. Arch. Orthop. Trauma Surg. 135 (8), 1101–1106. https://doi.org/10.1007/s00402-015-2252-4.

Yang, A.L., Mao, W., Chang, S.M., He, Y.Q., Li, L.L., Li, H.L., Long, F., Dong, Y.H., 2023 May. Computational evaluation of the axis-blade angle for measurements of implant positions in trochanteric hip fractures: a finite element analysis. Comput. Biol. Med. 158, 106830. https://doi.org/10.1016/j.compbiomed.2023.106830.

Zani, L., Cristofolini, L., Juszczyk, M., et al., 2012. In-vitro strain distribution during sideways fall in the proximal human femur. J. Biomech. (Suppl. 1)45, S351. https://doi.org/10.1016/j.jbiomech.2015.02.022.